

**FRACTAL GEOMETRY, IMAGE ANALYSIS & THERMAL PROFILING AS
QUANTITATIVE APPROACHES IN REDEFINING STAGING TIME AND FLOOR
LIFE OF NANOPARTICLE SILVER SINTER PASTE**

Marty Lorgino D. Pulutan, Janice M. Estolano, Maria Sandra A. Brucelo

Backend Technologies

Ampleon Philippines, Inc., Light Industry & Science Park I, Brgy. Diezmo, Cabuyao City, Laguna
marty.lorgino.pulutan@ampleon.com

ABSTRACT

The fractal pattern, geometrical structures and thermal responses of sintered nano Ag staged at varying window time between dispensing and paste curing were analyzed and measured through fractal geometry, image and thermal analyses to define maximum staging time and potential shelf life extension of the material. The complexity of sintered Ag pattern was inspected using SEM imaging of cross-sectioned samples and were correlated with homogeneity, translational invariance, particle, pore and resin distribution, sinter density, and sintered Ag and cured resin network and connection as a metric for delamination risk and propagation and sintering quality against varying staging times. The bleed out (BO) propagation was correlated with staging time using model fitting to predict maximum bleed out length and saturation point. Thermal analysis using DSC-TGA was done to check the behavior of staged pastes to check for characteristic peaks which may be associated with premature curing or early outgassing. Moreover, fractal parameters such as Lacunarity (Λ), Minkowski – Bouligand Dimension (D_B), porosity, pore shape factor (PSF) and pore size distribution (PSD) were measured using image analysis freeware to differentiate sinter structure and determine the effect on reliability of prolonged staging at ambient condition of the paste material. Results show prominent exothermic peak at 132 to 141 °C is detected associated to volatile outgassing and an inverse relationship between percent weight loss and staging time is observed indicating increased outgassing with prolonged staging time. Such findings agree with BO propagation which shows increased length from 24th until 84th hour mark. On the other hand, the fractal parameters Λ and D_B showed increasing and decreasing values respectively indicating that increase staging time affects the sinter structure by inducing non-uniformity triggered by premature sintering. Moreover, the porosity, PSF and PSD suggest increase in heterogeneity and non-homogeneity along the bondline of the sintered structure and is limited only until the 48th hour mark. Finally, the maximum staging time for the nano pure Ag sinter can be further prolonged up to 48 hours, thereby extending the shelf life through a cumulative consideration of thawing time and the interval between thawed glue and dispensing.

1. 0 INTRODUCTION

Sintering technology using Ag particles have gained attention in the recent years and was successfully introduced in the semiconductor and assembly of power electronics due to its high homologous temperature and compliance with Restrictive of Hazardous Substances (RoHS). The Ag sinter die attach material is commonly categorized into two types: pure and hybrid. Pure types, often referred to as pastes, consist mainly of Ag fillers, low-molecular solvents, and diluents. In contrast, hybrid types include epoxy resin, which fills in the pores and microvoids creating resin-reinforced system between sintered particles then cures simultaneously with the sintering of Ag particles. These types are further divided based on the size of Ag fillers used: micron or nano. Micron-sized fillers are typically employed in hybrid epoxy formulations, while nano-sized fillers are frequently formulated with solvents alone to enable further densification, resulting in significantly lower porosity compared to the other type. Although hybrid Ag sinter are deemed beneficial in packages that undergoes high thermomechanical stresses due to high CTE mismatches, pure types are preferred for those which requires higher power application that needs high thermal and electrical conductivity.

Ag nanoparticles have the tendency to self-sinter even without applied pressure once capping agents are removed [1]. And as a coherent property, nanoscale particles have the tendency to form agglomerates and aggregates [2, 3]. Agglomerates are considerably tolerable as it is easier to be dismantled by plain mechanical force while aggregates are harder to be re-dispersed because of its stronger metallic bond force that holds the particulates together [3, 4]. Aggregates could hinder the sintering process of the paste as well its reliability because it reduces densification rate along the process by reducing driving force [3 - 6]. The susceptibility of pure nano Ag sinter types to premature sintering is primary triggered by the staging time starting from thawed condition until just before loading for die attach curing.

Minimizing staging time is held necessary to avoid exceeding the maximum floor life of 24 hours as often outlined in the

material datasheet. However, adhering to such restriction poses a challenge during assembly, requiring measures to prevent excessive wastage of the die attach material and mitigate potential reliability failures and issues. Conventional approaches to revising staging duration and floor lifespan typically entail the use of Scanning Acoustic Microscopy (SAM) to assess interfacial integrity, which is commonly considered the main criterion for detecting delamination. Moreover, evaluating the quality of sintering structure often relies heavily on qualitative assessment, primarily through cross-sectional imaging without measurable data for comparison. In this study, the researchers defined staging time for a particular pure nano silver sinter paste material through fractal geometry, image analysis and thermal profiling.

2.0 REVIEW OF RELATED WORK

The sintered Ag structure consists of a network formed through the progressive growth and transformation of particles, involving surface diffusion, grain boundary migration, lattice diffusion, and eventual solid-state fusion [5, 7]. Particle growth follows the Ostwald Ripening mechanism, which describes not only the growth of particles but also the development of pores between adjoining Ag particles. The mechanism describes the mass transport of smaller Ag particles with lower chemical potential to adjacent larger particle fusing into one creating a larger particle. As a consequence, the pores also increase in size but decrease in frequency. The porosity of the sintered Ag based on a cross-sectional image can then be calculated using equation below.

$$\varphi = \frac{A_{pore}}{A_{bulk}} \quad \text{Equation 1}$$

The cross-sectional images usually obtained through Scanning Electron Microscopy (SEM) or Transmission Electron Microscopy (TEM), are converted to binary images where A_{pore} corresponds to the total cross-sectional area occupied by pores while A_{bulk} is the total area of the sintered Ag matrix both expressed in pixels [8]. Moreover, the average size of the particles can be calculated using Particle Size Distribution (PSD) which uses different algorithms to individualize and distinguish Ag particles. Measuring the average particle size would describe the growth progression of Ag particle attributed to sintering. Additionally, another parameter being measured is the Pore Shape Factor (PSF) given by,

$$F = \frac{4\pi A}{p^2} \quad \text{Equation 2}$$

The equation gives value between 0 and 1 where values close to 1 denotes round-shape pore and values close to 0 indicates irregularity in shape. Previous accounts suggest that more irregularly shape pores are prone to stress concentrations and

thus serves as initiation of fracture [9]. The three discussed parameters are thus far the most employed method in describing the pore structural characteristics during sintering.

Meanwhile, as the sintered structure are considered spatial patterns with peculiar geometric texture, the sintering quality can be quantitatively described using fractal geometry and parameters. Lacunarity (denoted as Λ) is a fractal parameter which describes the fractal system texture through its heterogeneity and translational invariance. The lacunarity can be measured using the equation below,

$$\Lambda(r) = \frac{z_Q^{(2)}(r)}{[z_Q^{(1)}(r)]^2} \quad \text{Equation 3}$$

where,

$$z_Q^{(q)}(r) = \sum_M M^q Q(M, r) \quad \text{Equation 4}$$

The Q signifies Dirac probability function, M is the mass in pixels, and r is the radius of the gliding boxes. Higher value of lacunarity denotes larger and more gaps, and high non-symmetry and irregularity [10]. Such predictor is used in digital image analysis often used in medical, biological and Soil Physics. In this study, lacunarity was correlated to homogeneity of the sintered matrix across different sections of the die attach, heterogeneity of sintered Ag to pores and the distribution and irregularity of pores throughout the bondline. Another fractal predictor which could describe sintered Ag structure is the Minkowski-Bouligand Dimension (D_B) also known as box-counting dimension, which assesses the self-similarity and complexity of recognizable patterns. Higher D_B values signify high similarity and symmetry to which is related to the densification and homogeneity of sintered structure. Simplified expression for D_B is given by,

$$D_B(X) = \lim_{t \rightarrow 0} \left(3 - \frac{\log(V(\partial X \otimes Y_r))}{\log r} \right)$$

where V is the volume of the structure under consideration while Y_r is the Euclidian sphere with radius r [11]. The sintering quality which would be described by these predictors and parameters are mainly influenced by several factors including the staging time at ambient conditions.

The primary phenomenon observed during ambient staging of thawed Ag sinter paste is the emergence of bleed out (BO) which is a halo like stain exists around the periphery of the die-attach [12 – 14] primarily composed of solvents, thinning agents and other highly volatile dilute liquids. The removed components during bleeding potentially includes the capping agents and binders that causes aggregation and agglomeration when prematurely removed [1]. Consequently, the surface affinity and energy of nanoparticles are immensely reduced

as the presence of loosely clump masses prevents high densification, atomic bonding and mass transport leading to eventual early failures.

In this paper, the researchers focused on quantitative characterization of sintered structure of sintered Ag through fractal, image and thermal analyses, ultimately to define recommended staging time and floor life for the paste material.

3.0 METHODOLOGY

The Ag sinter paste material primarily composed of 5-10% hexanediol and approximately 95% Ag nanoparticle is obtained from a local supplier and is dispensed on Ag-plated Cu leadframe and bonded on a Si die with Ag backside metallization (BSM) using multi-chip die bonder machine. The staging time between dispensed paste going to oven loading for curing is illustrated on below diagram.

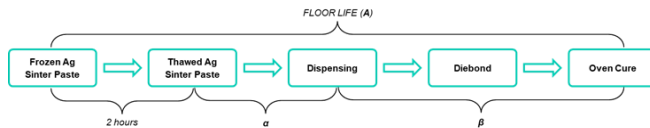


Fig. 1. Floor Life Diagram of Ag Sinter Paste From Frozen Until Before Cure.

The thawing time for the frozen paste is 2 hours following material supplier recommendation while the window time between the thawed paste going to dispensing α is kept as short as possible following the standard procedure for diebond process. The staging time β was varied based on the evaluation matrix below.

Table 1. Experimental Legs and Corresponding Staging Time From Dispensed Paste Going to Cure.

Leg No.	Thawing Time (Hours)	Staging Time α (Hours)	Staging Time β (Hours)
1	2	1	12
2	2	1	24
3	2	1	48
4	2	1	72
5	2	1	84
6	2	1	12, 24, 48, 72, 84

All specimens underwent curing according to the sintering profile recommended by the material supplier. One hundred units were assembled and molded for legs 1 to 5, while a

complete leadframe strip was die-bonded but did not proceed for molding and singulation as intended for leg 6.

3.1 Bleed Out Propagation Measurement

One-full strip was die bonded and the bleed out on top, bottom, left and right-hand side of each unit were measured using automated measuring system from 12th hour until 84th hour of staging. The average of bleed out on each unit side is plotted against increasing staging time and curve-fitted using Igor Pro software.

3.1 Thermal Profiling of Staged Pastes

Fifteen milligrams of paste were obtained from the sample at 12th to 84th hour of staging and the characteristic reaction peaks and percent weight loss were obtained using Simultaneous Thermal Analyzer (STA). The percent weight loss measurements were replotted against increasing staging time using Igor Pro software.

3.3 Fractal Geometry and Image Analysis

Thirty units each were pulled out from legs 1 to 5 at every readpoint – from 0-hour, post thermal cycling 500 cycles and post 1000 cycles. Each pulled out unit underwent the process as illustrated on below diagram.

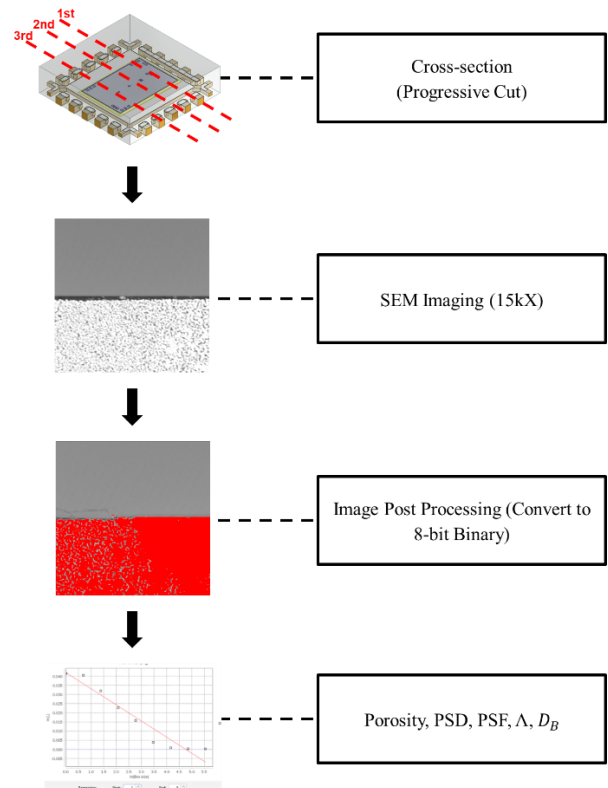


Fig. 2. Flow of Analysis for Fractal Geometry and Image Analysis.

The obtained samples were subjected for cross-section targeted on both sides near package peripheries and along the midsection based on Fig 2. The cross-sectioned samples were panned from end to end of the bondline subdivided into 5 sections (Fig. 3) using 15keV accelerating voltage and Backscattered Electron (BSD) detector to obtain images at 15kX magnification. All images were post processed and were converted into 8-bit binary images using image analysis portable freeware. For pore structure characterization, built-in plug-in were used to calculate porosity expressed in % area in pixels and PSF. Moreover, PSD utilized watershed algorithm to individualize Ag particles and average size were measured based on Feret's diameter.



Fig. 3. SEM Image of Sintered Ag Bondline Structure Subdivided Into 5 Sections as Used in Fractal Geometry and Image Analysis.

For Fractal Geometry Analysis, macros containing algorithm following Equation 4 and 5 were run to execute Λ and D_B measurement obtaining data sets replotted against increasing staging time using Igor Pro software.

4.0 RESULTS AND DISCUSSION

4.1 Effect of Staging Time on Bleed Out Propagation

The BO of the 100 uncured die bonded units were measured and the average on top, bottom, left and right-hand side were plotted against increasing staging time as shown in Fig. 4.

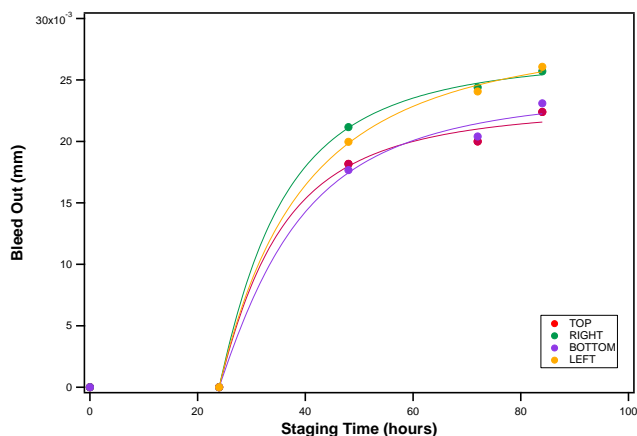


Fig. 4. Average BO Length Against Increasing Staging Time. Curve-fitting was done using Igor Pro software.

During the first 24 hours of staging under ambient conditions, no organic bleed out is observed on the peripheries of the uncured bonded paste. BO started to emerge after 48 hours at an average of 0.020 mm and gradually increased until 84th hour at an average of 0.025 mm. Gaussian curve fitting suggests that maximum BO of 0.025 mm is attained at 84th

hour mark where plateau of the curve is observed. Maximum BO is not deemed detrimental in diebond as the tightest die-to-die clearance is 250 μ m. However, the BO propagation suggests that phenols and potentially undeclared low-molecular volatile components are being removed from the dispensed paste and may significantly affect the sintering process by reducing the driving force due to the presence of agglomerates and aggregates [1-3]. The diminishing behavior of solvents and volatiles is further discussed in section 4.2.

4.2 Effect of Staging Time on Solvent Outgassing and Premature Sintering

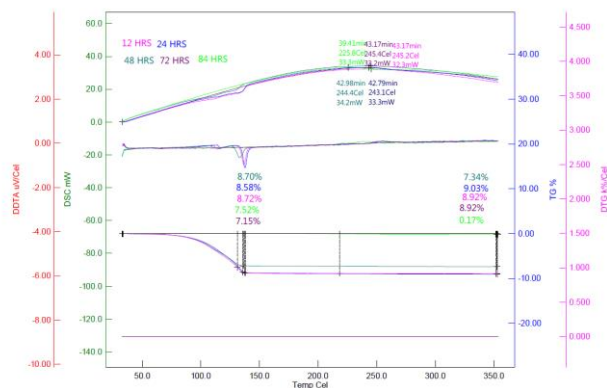


Fig. 5. STA Plot of Samples Staged at Varying Times Using 5degC/min From 30 to 350°C.

A prominent endothermic peak is observed at approximately 132 to 141°C attributed to the outgassing and vaporization of majority of phenols and other volatile components in the paste formulation. Samples staged for less than 48 hours exhibit weight losses that are relatively similar, averaging around 8.7% which corresponds to the total solvent and low-molecular volatile compounds complementing the declared composition of the material. The presence of these organic substances evolving within that temperature range implies that these components are designed to persist within the formulation until the curing process, as their vaporization typically takes place during the ramp-up stage before sintering, possibly serving to loosely bind the particles and prevent aggregation. Conversely, samples staged for more than 48 hours exhibited notably reduced weight loss with a delta of approximately 1.5%, suggesting that this amount had already been removed through prolonged exposure to ambient temperature. The removal of 1.5% of organic compounds during staging could have a notable impact on the resulting sintered structure, a topic that will be explored further in the subsequent sections.

4.2 Effect of Staging Time on Sintered Structure and Texture

4.2.1 Pore Structure Characterization

Porosity in percentage of area of detected pores (foreground) over total area occupied by the region of interest (ROI) (foreground + background) both expressed in pixels were measured using image analysis software and the averages are plotted against increasing staging time as shown in Fig. 4.

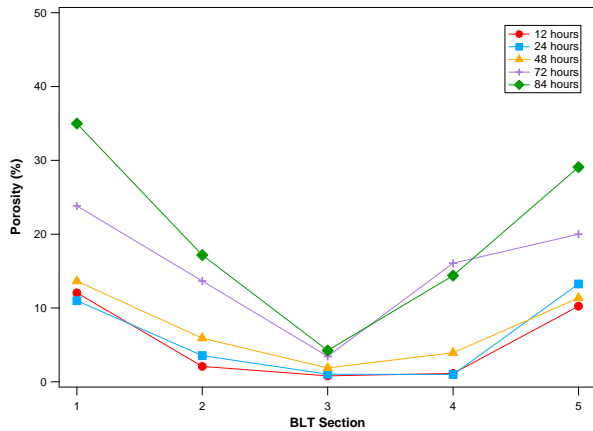


Fig. 6. Average Porosity Measured From End to End of Sintered Ag Bondline Against Increasing Staging Time.

The porosity values near sintered fillet are significantly higher than the rest of the sintered bondline section for all samples as governed by venting route factor of outgassing [11, 15]. Delamination between the porous fillet and the die pad surface is observed for all staged samples which are acceptable per defined criteria under the assumption that no propagation underneath the die occur. However, increased staging time at ambient condition triggered increase in porosity on sections 2 to 4 which are situated near midsection of the sintered structure for samples staged more than 48 hours and were observed to exhibit delamination as early as precondition as shown in Fig. 7.

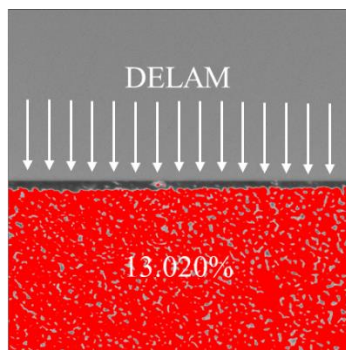


Fig. 7. SEM Image Post TMCL 1000 Taken at 15kX Focused on Section 2 of the Sample Staged for 72 Hours.

Porous zones with porosity higher than 10% were observed to fail after subjecting to thermal cycling. Such findings agree with the separate studies made by Chen and Wang [11, 15] where it can be deduced that the venting route taken by outgassing volatiles have created weak interface with the die BSM or with die pad surface and eventually delaminates

upon subjecting to thermomechanical stress. As such, samples which are staged less than 48 hours show porosity less than 10% and are likely to pass high number of thermal cycles. To assess the circularity of the pores detected on the porous zones, PSF per BLT section is presented in Fig. 8.

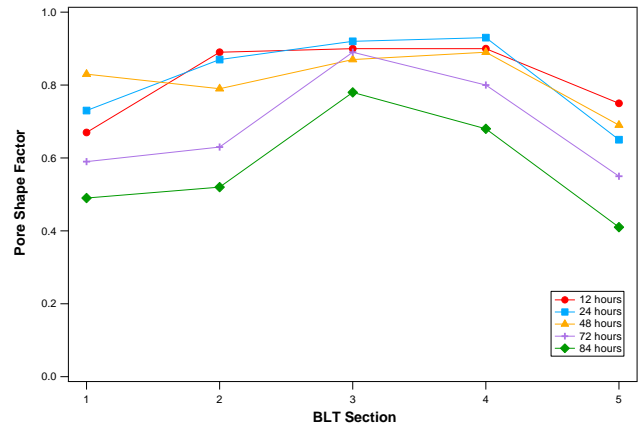


Fig. 8. Average Pore Shape Factor of Detected Pores From Different BLT Sections.

Using Equation 2, the circularity and irregularity of pores in average were measured based on calculated perimeter and area in pixels detected through Watershed Algorithm. Irregularly shaped pores are detected on fillet due to interconnected pores. The network of pores served as hotspots for fragility and consequently triggers crack formation and propagation originating from the fillet towards the interfaces [16]. Along with high porosity on such sections, the irregularly-shaped pores tortuously provide weak path for stress concentrations leading to cohesive or adhesive failure especially during reliability [9]. For samples staged more than 48 hours, the PSF are significantly lower based on pairwise posthoc comparison on all sections implying higher risk of crack or delamination at OH and post reliability. The pore size distribution is then measured using the same algorithm and based on Feret's diameter per individualized foreground particle detected.

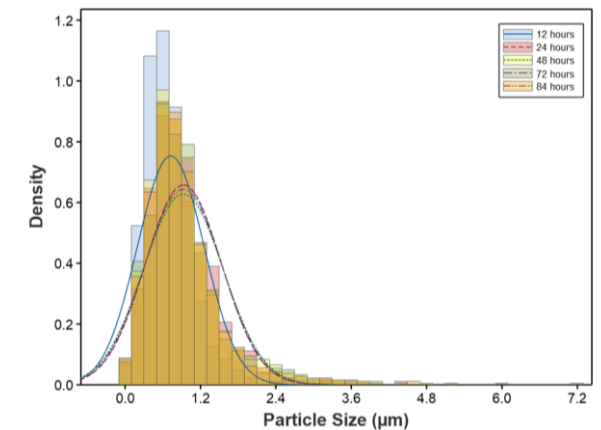


Fig. 9. Pore Size Distribution Against Varying Staging Time. The ROI's for the measurement were focused on section 2 and 4 of the sintered structure.

Based on Fig. 9, higher density and mode at 0.4 to 0.6 μm is observed for samples staged until 12 hours whereas at 0.6 to 0.8 μm for samples staged for and more than 24 hours. The results imply that shortest possible staging not exceeding the floor life would yield smaller pores thus higher densification. However, no significant difference was detected among all samples beyond 1.0 μm -size possibly due to necks between pores serving as partition for the algorithm to singulate from each other. The Feret's diameter thus did not consider the interconnection among pores and could be considered more conservative method in detection of highly irregular and elongated pores.

4.2.2 Fractal Geometry and Sintered Structure Texture Recognition

As discussed previously, sintered Ag structure highly resembles fractal pattern as it shows unique spatial pattern that could be described by fractal parameters. Using Equation 3, the Λ at varying r of gliding boxes was calculated for each sample staged at varying times.

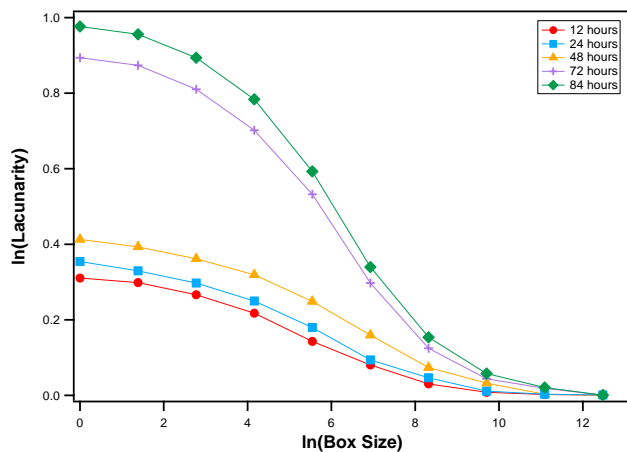


Fig. 10. Lacunarity Against Increasing Box Size of Samples Staged at Varying Times. The plot presents lacunarity calculated on section 2 of the BLT from each experimental leg.

The plot shows that at smallest box size r , the Λ increases with increasing staging time. The Λ measurements of samples staged between 12 and 48 hours exhibited closely clustered values, ranging from 0.32 to 0.41. A significant disparity and a leap in Λ was observed for samples staged for 72 and 84 hours indicating increase gaps and translational invariance which indicates increase in porosity and heterogeneity difference on different regions on section 2 of the BLT scanned by the gliding box. The increase in heterogeneity difference practically implies non-uniformity of pore to sintered structure distribution triggered by concentration of pores near fillet and near interfaces. On the other hand, samples staged less than 48 hours indicate lower

porosity thus higher densification and sintering. The low Λ on different ROI's on section 2 indicates low risk of stress concentration thus less risk of failure. The obtained values scanned by smallest to midsize r suggests that paste should be staged to maximum 48 hours to promote grain growth, densification and lower porosity.

The last fractal parameter used in the study is the Minkowski – Bouligand dimension (D_B) measured throughout the bondline of samples and plotted against increasing staging time as presented in Fig. 11.

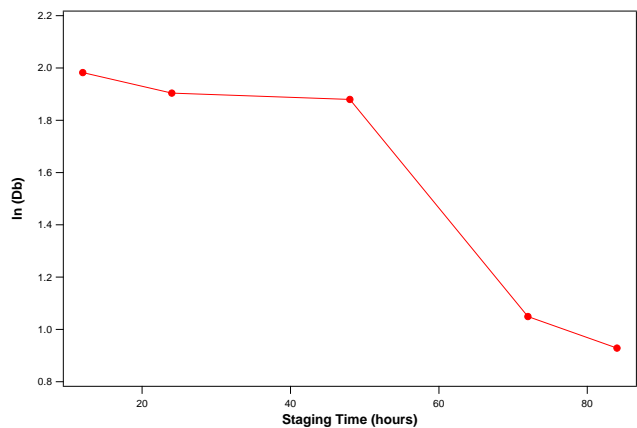


Fig. 11. Minkowski – Bouligand Dimension Against Increasing Staging Time. The plot presents D_B calculated from end-to-end of BLT from each experimental leg.

A sharp decline in D_B is observed after staging more than 48 hours which suggests increased asymmetry across the bondline of the sintered Ag structure. High D_B for samples staged less than 48 hours indicates high self-similarity which implies uniformity from end-to-end of the bondline. The pronounced uniformity observed in less staged samples is attributed to high sintered particle, resulting in minimal porous areas that closely resemble the entire bondline. Conversely, the notably lower D_B in samples staged more than 48 hours is due to localized pores found in various sections of the bondline, particularly concentrated near the ends. Overall, the D_B suggests that staging less than 48 hours would allow sintered structure to be more uniform as well as the porosity distribution. In the case of less staged samples, the absence of porous zones underneath the die triggered high self-similarity of the overall bondline which corresponds to higher D_B

5.0 CONCLUSION

In summary, the quantitative approaches utilized in the study particularly fractal geometry, image analysis and thermal profiling were successfully employed to characterize the pore and sintered structure and were correlated with increasing staging time. The measurements of BO and dynamic STA indicate that longer staging times under ambient conditions

prompted the separation of volatile components in the dispensed paste through BO propagation and room temperature outgassing, consequently leading to the formation of agglomerates and aggregates. On the other hand, pore structure characterization suggests increased porosity, lower circularity, and higher density on larger pores with increasing staging time. Additionally, the fractal parameters Λ and D_B indicates that porosity increases with non-uniform distribution of sintered structure to pore per section throughout the bondline. Overall, the results suggest that increased staging time to ambient temperature triggers separation of critical phenols and other capping agents in the paste which allows formation of aggregates and agglomerates. The presence of such clump of masses lowers the driving force of nanoparticles to sinter during exposure to high temperature thus creating high porosity zones which are highly irregular in shape. The outgassing of volatiles prior sintering step also weakens the interfaces above porous zones which delaminates further on during thermal cycling. The non-uniform distribution of sintered network to pores providing high heterogeneity along with non-uniformity across bondline are primarily triggered by prolonged staging which eventually fails during reliability. Lastly, the staging time between dispensed paste going to oven cure for the particular nanoparticle Ag sinter paste material used in the study could be extended for 48 hours. As such, the floor life of the material could also be extended cumulatively with thawing time and the window time between thawed glue going to dispensing.

6.0 RECOMMENDATIONS

The researchers recommend to explore percolative parameters to quantify the connectedness of the sintered network. Mathematical models using the measured porosity can also be used to predict elastic modulus of the sintered structure as staging time increases. Additionally, the efficacy of the proposed quantitative approaches could be further confirmed by testing other types of Ag sinter die attach materials, such as hybrids or epoxies, along with pastes containing micro-sized particles. Lastly, correlation with test responses such as conductivity and its effect with prolonged staging time is a potential avenue for future study.

7.0 ACKNOWLEDGMENT

The authors wish to extend their deepest appreciation to the engineers and technicians at the Backend Technologies Competence Center for their assistance in conducting the experiments, to Jerome Amado for providing valuable insights and guidance to enhance the study, and to the management team of Ampleon Phils. Inc. for their support, which was instrumental in facilitating this research.

8.0 REFERENCES

1. K. S. Siow, *J. Electron. Mater.*, 43(4), 2014, 947-961.
2. W. Guo, et al, *J. Nanomater.*, 2015, 1-7.
3. N. M. Noordin, & K. Y. Cheong, *Procedia Eng.*, 184, 2017, 611-615.
4. K. S. Siow, *J. Alloys Compd.*, 514, 2012, 6-19.
5. V. R. Manikam, & E. N. Tolentino, *16th EPTC.*, 2014.
6. L. A. Navarro, et al., *Ingen. Mecan. Tecnol. Y Desarr.*, 4(3), 2012, 97-102.
7. S. Zhao, et al., *2015 ICEP-IAAC*, 2015.
8. C. Chen, & K. Suganuma, *Mater. Des.*, 162, 2019, 311-32117
9. Y. Kim, et al., *Mater. Today Commun.*, 29, 2021, 102772.
10. C. Allain, & M. Cloitre, *PRA*, 44(6), 1991, 3552-3558.
11. Y. Wang, et al., *Mol. Cryst. Liq. Cryst.*, 604(1), 2014, 11-26.
12. J. Hsiung, et al., *J. Adhes. Sci. Technol.*, 17(1), 2003, 1-13.
13. M. Burmeister, et al., *38th Int. Sympo. Micro.*, 2005, 771-778.
14. B. Neff, et al., *Int. Sympo. Adv. Packag. Mater.* 2005.
15. S. Chen, *16th ICEPT*, 2015.
16. K. Sasaki, *63rd ECTC*, 2013.

9.0 ABOUT THE AUTHORS

Marty Lorgino D. Pulutan received the B. S. degree in Applied Physics specializing in Materials Physics from University of the Philippines, Los Baños in 2017 and currently pursuing M. S. degree in Materials Science and Engineering by Research in Mapua University. He has published a total of 10 papers in peer-reviewed journals and international conference proceedings. He is currently a Senior Materials Development Engineer under Back End Technologies Department in Ampleon Philippines, Inc.

Janice M. Estolano received the B. S. degree in Computer Engineering in AMA Computer College, Alangilan, Batangas in 2022. She is currently a Senior Materials Development Technician under Back End Technologies Department in Ampleon Philippines, Inc.

Maria Sandra A. Brucelo received the B. S. degree in Business Administration specializing in Business Management from Trimex Colleges, Biñan in 2022. She is currently a Materials Development Technician under Back End Technologies Department in Ampleon Philippines, Inc.

